Stereoselectivity

DOI: 10.1002/anie.201001588

Enamine versus Oxazolidinone: What Controls Stereoselectivity in Proline-Catalyzed Asymmetric Aldol Reactions?**

*Akhilesh K. Sharma and Raghavan B. Sunoj**

The progressively larger number of reports on the success of organocatalysis in the current decade indicates the unprecedented growth in this area.[1] Comprehensive accounts of an assortment of organocatalytic reactions are now available.[2] Among the plethora of organocatalysts, amines, diamines, and other related bifunctional organic molecules continue to receive great attention from organic chemists.[3] The applications of reactions catalyzed by proline are so many that it could now be regarded as a prototypical example of an organocatalyst.[4]

The efficiency of proline in asymmetric catalysis is largely attributed to its bifunctional characteristics as well as to the presence of a chiral center.[2a,e,4d] Experimental reports focusing on the mechanism of organocatalytic reactions were relatively scarce until very recently.[5] Significantly, there has already been sufficient debate over the mechanism of proline-catalyzed reactions.[6] Some of the most pertinent issues include whether one or two molecules of proline are involved, or if an enamine or a bicyclic oxazolidinone intermediate holds the key to the mechanism. While the former proposition has been settled through kinetic experiments,[5f] the cogitations on the latter remain prevalent.[7] There have been interesting studies, such as NMR spectroscopic evidence on the participation of oxazolidinone intermediates in proline-catalyzed aldol reactions.[5c,d,6,8] Both catalytic and parasitic roles[9] of oxazolidinones have been proposed.[5d,7] On the other hand, the detection of putative enamine intermediates of unactivated carbonyl compounds in aldol reactions continues to pose formidable challenges. A recent ESI mass spectrometry study, however, endorses the view that the aldol reaction proceeds through a proline–enamine pathway.[10]

A perusal of recent developments readily reveals that the synergism between experimental and computational studies in proline-catalyzed asymmetric reactions has been timely and effective. In particular, the concurrence between the predicted stereochemical outcome obtained by using density functional methods and the corresponding experimental observations in organocatalytic reactions has been quite impressive.[11] While the mechanistic conformity, or even parallelism, between the enamine and oxazolidinone pathways appears to demand further studies, we intend to emphasize a more critical issue of stereoselectivity at this juncture. The key premise on which most of the proline-catalyzed stereoselective reactions are rationalized rests with the enamine model of Houk and List. In the Houk–List model, the stereoselectivity is proposed to arise in the C–C bond-formation step between an enamine (derived from proline and suitable carbonyl compounds) and an electrophile (Scheme 1). As part of our ongoing research efforts in asymmetric organocatalysis,[12] we have chosen to examine the stereoselectivity in the proline-catalyzed self-aldol reaction of propanal, in light of the recently proposed oxazolidinone pathway. In an earlier study, MacMillan and co-workers reported high levels of stereocontrol of the order of 99% enantiomeric excess and *anti* diastereoselectivity (4:1 *anti*:*syn*) for the same reaction.[13] We primarily employed density functional and ab initio MP2 computations in this study.[14] The discussions are presented on the basis of the B3LYP/6-31+G** results.

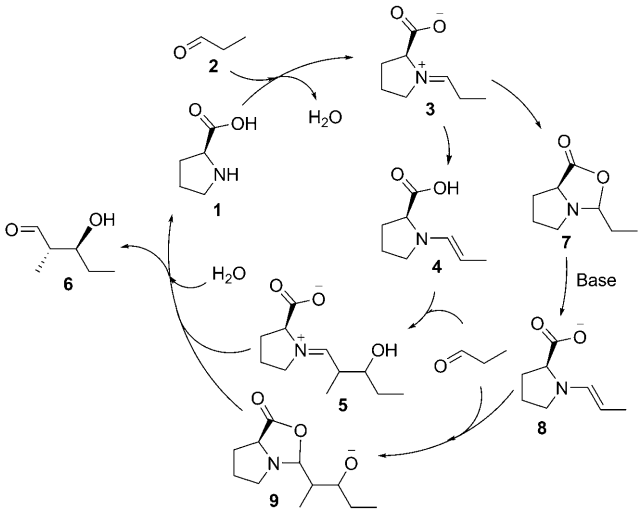

Scheme 1. Important mechanistic possibilities involving the enamine and oxazolidinone pathways for the proline-catalyzed self-aldol reaction of propanal.

The mechanism of the proline-catalyzed aldol reaction is proposed to involve a number of intermediates, as shown in Scheme 1. The catalytic cycle can be envisaged to begin with the formation of iminium carboxylate (**3**) from propanal (**2**) and proline (**1**). The intermediate **3** can convert either to an

[*] A. K. Sharma, Prof. Dr. R. B. Sunoj
Department of Chemistry
Indian Institute of Technology Bombay
Powai, Mumbai 400076 (India)
Fax: (+91) 22-2576-7152
E-mail: sunoj@chem.iitb.ac.in
Homepage: http://www.chem.iitb.ac.in/~sunoj

[**] We thank IIT Bombay computer center and CMSD Hyderabad for generous computing time. A.K.S. is grateful to CSIR New Delhi for a senior research fellowship.

Supporting information for this article is available on the WWW under http://dx.doi.org/10.1002/anie.201001588.

enamine carboxylic acid (**4**) or to an oxazolidinone intermediate (**7**). On the basis of the orientation of the ethyl moiety with respect to the carboxylate group, both *E* (**3a**) and *Z* (**3b**) isomers are identified.[15] The barrier for the formation of **7** by the intramolecular attack of the carboxylate on the iminium is found to be very small.[16] Furthermore, this process is thermodynamically more favored than the formation of **4**. More importantly, the barrier for the reversal of **7** to **3**, that is, oxazolidinone ring opening, is relatively larger. For instance, these barriers are 12.8 and 17.6 kcal mol^{-1} for **7a** (*endo*) and **7b** (*exo*), respectively (Figure 1).[17]

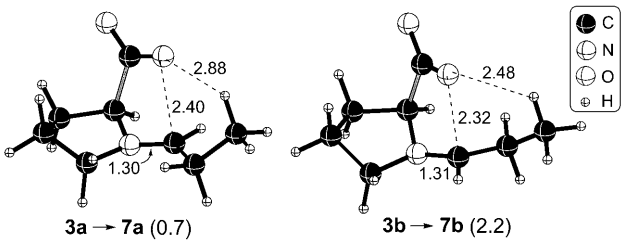

Figure 1. Transition states (TSs) for oxazolidinone (**7**) formation from iminium carboxylate. The Gibbs free energy of activation [kcal mol^{-1}] is given in parentheses; bond lengths are in Å.

The computed energetic details evidently suggest an equilibrium composition in favor of the oxazolidinone intermediate.[18] This could therefore be regarded as the major reason for being able to detect oxazolidinones over other putative intermediates, such as the iminium ion and enamine, in proline-catalyzed direct aldol reactions.[6,7,8c] Among the resulting oxazolidinones, **7b** is more stable than **7a** by 2.1 kcal mol^{-1}. Two related processes emanating from the key intermediate iminium carboxylate are the formation of enamine carboxylic acid (**4**) as well as enamine carboxylate (**8**). Different scenarios depicted in pathways 1–3 in Scheme 2

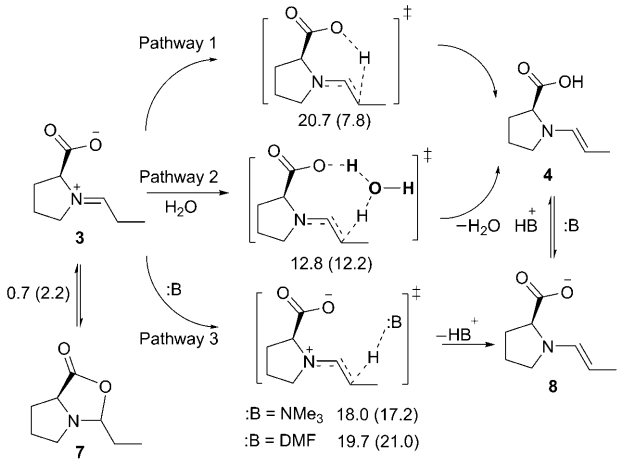

Scheme 2. Different possibilities for the conversion of iminium carboxylate **3** to various other key intermediates. The Gibbs free energy of activation [kcal mol^{-1}] for the reaction of **3a** is provided along with that for **3b** in parentheses.

are considered. Pathways 1 and 2 represent the unassisted and water-assisted conversion of **3** to **4**, respectively.[19] While **3b** to **4b** (*syn*) conversion can take place without the involvement of water, the geometric feature of **3a** clearly demands an assisted proton transfer to afford **4a** (*anti*).[20] In fact, water-assisted tautomerization of **3b** to **4b** is about 4 kcal mol^{-1} higher than the corresponding unassisted pathway.

The availability of **4** and **7** can lead to an interesting mechanistic divergence, capable of exerting a direct influence on the stereochemical outcome of the reaction. The presence of **4** could facilitate the commonly employed Houk–List mechanism, whereas **7** could result in the Seebach oxazolidinone pathway. Both these C–C bond-formation pathways are examined herein. Notably, in the Houk–List pathway the barrier for rotation around the C–N bond in **4** is about 6.9 kcal mol^{-1}. Involvement of both **4a** and **4b** enamines in the C–C bond formation is therefore likely. The addition of enamine **4a** to propanal is found to be more preferred over that involving enamine **4b**.[21] A more important aspect at this juncture relates to the predicted stereochemical outcome of the reaction. The computed relative energies of the diastereomeric transition states **TS(4a–5a)***re–re* and **TS(4a–5a)***re–si* clearly indicate that the diastereoselectivity, as summarized in Table 1, is in good agreement with the experimental results. Furthermore, the predicted product configuration (2*S*,3*S*)-3-hydroxy-2-methylpentanal is also in line with the available reports.[13,22]

Table 1: Gibbs free energy of activation[a] [kcal mol^{-1}] for C–C bond formation at different levels (L1–L5) of theory in the Houk–List pathway.

TS(4→5)[b]		L1	L2	L3	L4	L5
4a→5a	*re–re*	23.6	20.5	16.1	21.6[d]	15.4
	re–si	24.6	21.4	16.2	22.0	15.1
4b→5b	*si–si*	27.0	24.0	19.5	25.3	18.3
	si–re	28.0	24.8	21.0	24.8[d]	19.5
	re–si	32.2	29.2	25.3	32.2	24.6
	re–re	33.6	30.9	27.1	34.3	26.1
Computed	% *ee*	>99	>99	>99	>99	98.5
selectivity	*anti*:*syn*	5.4:1	4.6:1	1.2:1	2:1	1:1.7
Experimental selectivity[c]	99% *ee* *anti*:*syn* = 4:1					

[a] Computed with reference to **4a** and propanal. L1 = B3LYP/6-31 + G**, L2 = mPW1PW91/6-31 + G**, L3 = MP2(FULL)/6-31 + G**//6-31G*, L4 = IEF-PCM$_{CH3CN}$/B3LYP/6-31 + G**, L5 = M05-2X/6-31 + G**. [b] The stereochemical notations (*re*/*si*) represent the prochiral faces of enamine and propanal, respectively. [c] Values taken from reference [13]. [d] Single-point calculations on the gas-phase geometries for all species, as full optimizations of this TS could not be carried out in the condensed phase.

In the Seebach pathway, an enamine carboxylate **8** is proposed to function as the key reactive intermediate. Multiple possibilities for the generation of **8** as depicted in Scheme 2 are examined.[23] The vital stereodifferentiation in C–C bond formation in the Seebach model is suggested to occur when **8** reacts with the electrophile. This step consists of a *trans* addition of the carboxylate oxygen atom on the enamino C=C bond and the concomitant formation of a new C–C bond with the electrophile. The geometries of the

transition structures suggest an asynchronous and late TS, in which C–C bond formation is found to be ahead of the oxazolidinone ring closure.

Depending on the relative positions of the developing alkoxide oxygen atoms with respect to the enamino C=C bond in **8**, three TS geometric possibilities are identified. These are represented as $TS_{60/180/300}$ along with the corresponding prochiral faces of **8** and the incoming electrophile. In the case of addition of **8a** (*anti*), **TS(8a–9a)***si–re*$_{(300)}$ is identified as energetically the most preferred as compared to the other likely rotamers around the developing C–C bond (Table 2). In this TS, the hydrogen-bonding interaction

Table 2: Gibbs free energy of activation[a] [kcal mol^{-1}] for C–C bond formation at different levels (L1–L5) of theory in the Seebach pathway.

TS(8→9)[b]		L1	L2	L3	L4	L5
8a→9a	*si–re*$_{(60)}$	35.9	29.7	24.4	–[c]	26.2
	si–re$_{(180)}$	37.3	30.8	24.9	44.5	27.4
	si–re$_{(300)}$	35.2	28.6	22.4	44.6	24.6
	si–si$_{(60)}$	36.6	30.5	24.1	43.5	26.1
	si–si$_{(180)}$	36.0	29.6	24.1	42.5	26.4
	si–si$_{(300)}$	36.2	29.6	23.3	–[c]	25.0
8b→9b	*re–re*$_{(60)}$	40.9	34.7	28.3	–[c]	30.7
	re–re$_{(180)}$	38.2	32.5	27.1	50.0	29.8
	re–re$_{(300)}$	37.7	32.1	25.9	50.1	28.2
	re–si$_{(60)}$	39.9	33.9	27.6	–[c]	30.2
	re–si$_{(180)}$	38.9	31.9	27.7	51.5	30.4
	re–si$_{(300)}$	37.4	33.0	26.2	49.8	27.8
Computed	ee%	95	>99	>99	–[d]	>99
selectivity	*anti*:*syn*	1:3.9	1:5.4	1:4.6	–[d]	1:2

[a] Computed with reference to **8a** and propanal. [b] The stereochemical notations (*re*/*si*) employed for the TSs represent the prochiral faces of enamine carboxylate and propapal, respectively. L1 = B3LYP/6-31+G**, L2 = mPW1PW91/6-31+G**, L3 = MP2(FULL)/6-31+G**//6-31G*, L4 = IEF-PCM$_{CH3CN}$/B3LYP/6-31+G**, L5 = M05-2X/6-31+G**. [c] Full optimizations of this TS could not be carried out in the condensed phase. [d] All required values are not available.

between the developing alkoxide and the Cα′-H of the pyrrolidine ring appears to help gain improved stabilization (**I** in Figure 2).[24] Among the *si–si* mode of additions, **TS(8a–9a)***si–si*$_{(180)}$ is relatively more preferred. In general, the barrier for the addition of **8b** (*syn*) is found to be higher than those involving **8a** (*anti*). For instance, the energy difference between the addition of **8a** and **8b**, given by **TS(8a–9a)***si–re*$_{(300)}$ and **TS(8b–9b)***re–si*$_{(300)}$, respectively, is more than 2 kcal mol^{-1} at the B3LYP level and even larger at other levels of theory considered here.

The computed Gibbs free energies of activation for C–C bond formation in the oxazolidinone pathway are provided in Table 2. Interestingly, the barriers are found to be larger than that in the enamine pathway. The barriers in the oxazolidinone pathway are higher by 11.6 and 6.3 kcal mol^{-1}, respectively, at the B3LYP and MP2 levels of theory. The approach of the electrophile in the preferred lower-energy TSs is identified as occurring from the face opposite to the carboxylate group (*anti* addition). This is at variance with the Houk–List model, wherein the electrophile approaches from the same face as the carboxylic acid group of the

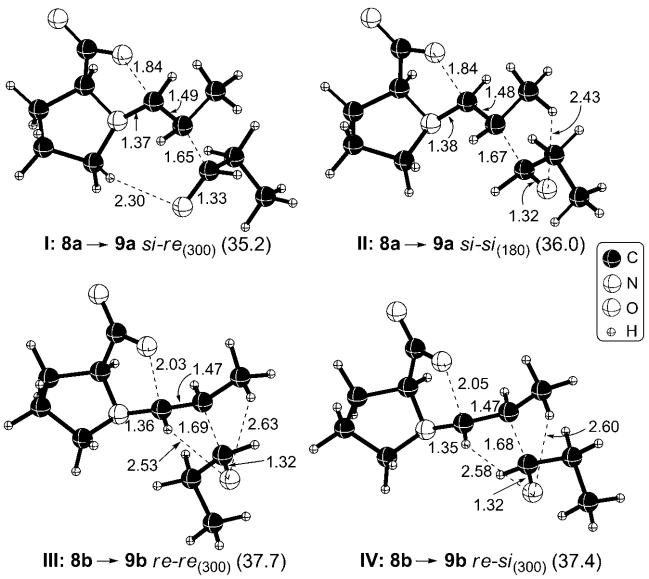

Figure 2. Optimized geometries of TSs for the stereoselectivity-controlling C–C bond formation in the Seebach pathway. The Gibbs free energy of activation [kcal mol^{-1}] is given in parentheses; bond lengths are in Å.

enamine.[25] In the most preferred mode, *anti* addition of the *si* face of **8a** to the *re* face of propanal is noticed.[26] The implication emerging from this analysis is a conspicuous kinetic preference for the *si–re* addition between **8a** and propanal. Readily noticeable is the configuration of the resulting stereoisomer as 2*R*,3*S*, which is exactly opposite to the stereochemical outcome predicted by using the Houk–List pathway.

The diastereomeric ratio computed using the activation barriers in the oxazolidinone pathway is 1:4 *anti*:*syn*, in favor of the *syn* diastereomer.[27] The diastereomeric composition predicted here is contrary to what has been shown experimentally.[13] Significantly, the conclusions are almost invariant at the different levels of theory employed in this work, which suggest the formation of the *syn* diastereomer as the major product. The lack of consensus between the experimental and computed product stereochemistries obtained by using the oxazolidinone pathway is traced to the preferred mode of addition between **8** and propanal. For example, the correct stereochemical outcome in the oxazolidinone pathway could arise from *anti* additions of 1) **8b** to propanal through **TS(8b–9b)***re–re*, and 2) **8a** through **TS(8a–9a)***re–re,* or the *syn* addition of 3) **8a** through **TS(8a–9a)***re–re.* However, these possibilities are higher in energy than the other lower-energy approaches discussed above.[28]

Apart from the kinetic factors hitherto described, the resulting oxazolidinone intermediate **9** is found to be notably higher in energy than the corresponding intermediate **5** in the enamine pathway obtained as a result of C–C bond formation (Figure 3). According to Seebach's proposal, **9b** (*exo*) should be more stable than **9a** (*endo*), which upon subsequent steps will yield an aldol product with the correct stereochemistry. While the computed energies do indeed indicate that **9b** is more stable (ca. 3–5 kcal mol^{-1}),[29] the associated barrier for

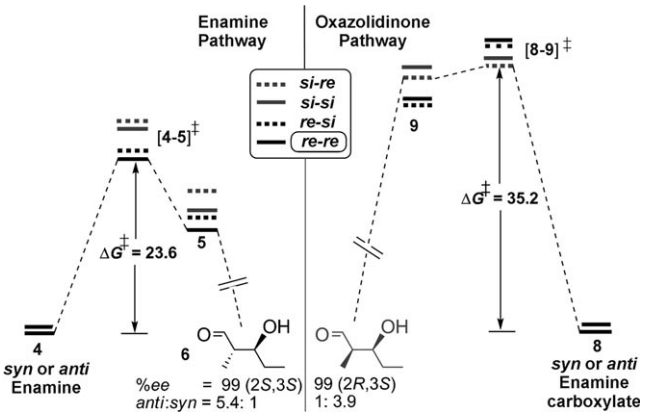

Figure 3. Free energy profile [kcal mol^{-1}] for C–C bond formation through enamine and oxazolidinone pathways.

its formation is evidently higher. The Gibbs free energy of activation, as given by **TS(8b–9b)***re–re*$_{(300)}$ leading to **9b**, is higher than that for **TS(8a–9a)***si–re*$_{(300)}$ responsible for **9a**, thus implying a kinetic preference toward **9a** oxazolidinone. The collective inference emerging from these factors is that even though the mechanistic scheme supports the formation of certain detectable intermediates, the computed energetics in the oxazolidinone model are not adequate to predict the correct stereochemistry of the major product.

In summary, the Houk–List transition model involving an enamine intermediate for stereoselective C–C bond formation in the proline-catalyzed self-aldol reaction of propanal is found to be effective toward rationalizing the experimentally observed enantio- and diastereoselectivities. The Seebach model involving an oxazolidinone intermediate is identified as inadequate for predicting the stereochemical outcome. Both enantio- and diastereoselectivities are at variance with the experimental results available for the title reaction. We propose that a convergence between the enamine and oxazolidinone pathways is likely under the experimental conditions employed, wherein the key intermediate enamine carboxylate (**8**) of the oxazolidinone pathway could merge with the enamine pathway through a protonation to yield proline enamine carboxylic acid (**4**).[30] Beginning with **4**, the stereochemical outcome of the reaction can be readily explained.

Experimental Section

Gas-phase calculations were performed at the B3LYP, mPW1PW91, M05-2X, and MP2(full) levels of theory.[31] For the density functional methods a 6-31 + G** basis set was used, and for the MP2(full) level a 6-31G* basis set was employed. The effect of solvent was included by using the integral equation formalism polarizable continuum model (IEF-PCM) in acetonitrile continuum. All calculations were performed using Gaussian 03.[32] Full details of the computational methods are provided in the Supporting Information.

Received: March 17, 2010
Revised: May 21, 2010
Published online: July 21, 2010

Keywords: aldol reaction · density functional calculations · diastereoselectivity · organocatalysis · reaction mechanisms

[1] D. W. C. MacMillan, *Nature* **2008**, *455*, 304–308.
[2] a) S. Bertelsen, K. A. Jørgensen, *Chem. Soc. Rev.* **2009**, *38*, 2178–2189; b) C. F. Barbas III, *Angew. Chem.* **2008**, *120*, 44–50; *Angew. Chem. Int. Ed.* **2008**, *47*, 42–47; c) A. Dondoni, A. Massi, *Angew. Chem.* **2008**, *120*, 4716–4739; *Angew. Chem. Int. Ed.* **2008**, *47*, 4638–4660; d) *Chem. Rev.* **2007**, *107*(12), special issue on organocatalysis; e) P. I. Dalko, L. Moisan, *Angew. Chem.* **2004**, *116*, 5248–5286; *Angew. Chem. Int. Ed.* **2004**, *43*, 5138–5175.
[3] a) S. Mukherjee, J. W. Yang, S. Hoffmann, B. List, *Chem. Rev.* **2007**, *107*, 5471–5569; b) G. Guillena, C. Nájera, D. J. Ramón, *Tetrahedron: Asymmetry* **2007**, *18*, 2249–2293; c) Z. Tang, F. Jiang, L.-T. Yu, X. Cui, L.-Z. Gong, A.-Q. Mi, Y.-Z. Jiang, Y.-D. Wu, *J. Am. Chem. Soc.* **2003**, *125*, 5262–5263.
[4] a) A. Ting, S. E. Schaus, *Eur. J. Org. Chem.* **2007**, 5797–5815; b) N. Vignola, B. List, *J. Am. Chem. Soc.* **2004**, *126*, 450–451; c) S. Saito, H. Yamamoto, *Acc. Chem. Res.* **2004**, *37*, 570–579; d) B. List, *Tetrahedron* **2002**, *58*, 5573–5590; e) B. List, *J. Am. Chem. Soc.* **2002**, *124*, 5656–5657; f) S. Hanessian, V. Pham, *Org. Lett.* **2000**, *2*, 2975–2978; g) A. Córdova, W. Notz, C. F. Barbas III, *J. Org. Chem.* **2002**, *67*, 301–303.
[5] a) N. Zotova, L. J. Broadbelt, A. Armstrong, D. G. Blackmond, *Bioorg. Med. Chem. Lett.* **2009**, *19*, 3934–3937; b) H. Zhu, F. R. Clemente, K. N. Houk, M. P. Meyer, *J. Am. Chem. Soc.* **2009**, *131*, 1632–1633; c) P. M. Phiko, K. M. Laurikainen, A. Usano, A. I. Nyberg, J. A. Kaavi, *Tetrahedron* **2006**, *62*, 317–328; d) A. Hartikka, P. I. Arvidsson, *Eur. J. Org. Chem.* **2005**, 4287–4295; e) H. Iwamura, D. J. Wells, Jr., S. P. Mathew, M. Klussmann, A. Armstrong, D. G. Blackmond, *J. Am. Chem. Soc.* **2004**, *126*, 16312–16313; f) L. Hoang, S. Bahmanyar, K. N. Houk, B. List, *J. Am. Chem. Soc.* **2003**, *125*, 16–17.
[6] B. List, L. Hoang, H. J. Martin, *Proc. Natl. Acad. Sci. USA* **2004**, *101*, 5839–5842.
[7] D. Seebach, A. K. Beck, D. M. Badine, M. Limbach, A. Eschenmoser, A. M. Treasurywala, R. Hobi, W. Prikoszovich, B. Linder, *Helv. Chim. Acta* **2007**, *90*, 425–471.
[8] a) Á. L. F. de Arriba, L. Simón, C. Raposo, V. Alcázar, J. R. Morán, *Tetrahedron* **2009**, *65*, 4841–4845; b) N. Zotova, A. Franzke, A. Armstrong, D. G. Blackmond, *J. Am. Chem. Soc.* **2007**, *129*, 15100–15101; c) H. Iwamura, S. P. Mathew, D. G. Blackmond, *J. Am. Chem. Soc.* **2004**, *126*, 11770–11771.
[9] Oxazolidinone has been known to be a parasitic dead end as it proposed to decrease the concentration of the active iminium ion. See references [5d] and [6].
[10] C. Marquez, J. O. Metzger, *Chem. Commun.* **2006**, 1539–1541.
[11] a) A. Fu, B. List, W. Thiel, *J. Org. Chem.* **2006**, *71*, 320–326; b) C. Allemann, R. Gordillo, F. R. Clemente, P. H.-Y Cheong, K. N. Houk, *Acc. Chem. Res.* **2004**, *37*, 558–569; c) F. R. Clemente, K. N. Houk, *Angew. Chem.* **2004**, *116*, 5890–5892; *Angew. Chem. Int. Ed.* **2004**, *43*, 5766–5768; d) S. Bahmanyar, K. N. Houk, *Org. Lett.* **2003**, *5*, 1249–1251.
[12] a) M. P. Patil, R. B. Sunoj, *Chem. Asian J.* **2009**, *4*, 714–724; b) C. B. Shinisha, R. B. Sunoj, *Org. Biomol. Chem.* **2008**, *6*, 3921–3929; c) M. P. Patil, R. B. Sunoj, *Chem. Eur. J.* **2008**, *14*, 10472–10485; d) C. B. Shinisha, R. B. Sunoj, *Org. Biomol. Chem.* **2007**, *5*, 1287–1294; e) M. P. Patil, R. B. Sunoj, *J. Org. Chem.* **2007**, *72*, 8202–8215.
[13] A. B. Northrup, D. W. C. MacMillan, *J. Am. Chem. Soc.* **2002**, *124*, 6798–6799.
[14] a) See the Supporting Information for full details of the computational methods. b) The B3LYP functional is known to be quite successful in studying stereoselectivity in organocatalytic reactions. For examples, see references [11a] and [12b] and

P. H.-Y. Cheong, K. N. Houk, *J. Am. Chem. Soc.* **2004**, *126*, 13912 – 13913.

[15] The energy of **3b** is only about 1.3 kcal mol^{-1} higher than that of **3a**. However, the barrier for conversion of **3a** to the corresponding *syn* geometry (via **7b**) is as high as 24 kcal mol^{-1}. See Table S2 and Figure S4 in the Supporting Information for further details.

[16] The barriers for the formation of **7** are 0.7 and 2.2 kcal mol^{-1}, respectively, for **3a** and **3b** iminium ions. The relative energies of the corresponding TSs with respect to the separated reactants are identified as 17.9 and 20.7 kcal mol^{-1}, respectively, for **3a** and **3b**.

[17] The *endo*/*exo* nomenclature is assigned on the basis of the orientation of the ethyl group with respect to the bicyclic oxazolidinone ring.

[18] A comparative energy profile diagram is provided in Figure S2 in the Supporting Information.

[19] a) Note that the generation of **3** from proline and propanal involves the release of a molecule of water in the dehydration step. b) We and others have earlier demonstrated the energetic advantages associated with water-assisted proton transfers in organocatalytic reactions. c) D. Roy, C. Patel, R. B. Sunoj, *J. Org. Chem.* **2009**, *74*, 6936 – 6943; d) F. J. S. Duarte, E. J. Cabrita, G. Frenking, A. G. Santos, *Chem. Eur. J.* **2009**, *15*, 1734 – 1746; e) D. Roy, R. B. Sunoj, *Chem. Eur. J.* **2008**, *14*, 10530 – 10534; f) F.-Q. Shi, X. Li, Y. Xia, L. Zhang, Z.-X. Yu, *J. Am. Chem. Soc.* **2007**, *129*, 15503 – 15512.

[20] a) The likely involvement of 1) water, 2) base, or 3) solvent in the assisted proton transfer is examined. b) The energetic information associated with these pathways is provided in Table S3 in the Supporting Information. The efficiency of these assisted processes is in the order H_2O > trimethylamine (NMe_3) > DMF.

[21] In the lower-energy TSs, the developing charge on the alkoxide moiety of propanal benefits from the stabilization offered by the carboxylic acid group. See Figure S6 in the Supporting Information.

[22] While the trends at different levels of theory by and large are similar and in concurrence with the experimental observations, the results obtained by using the M05-2X functional, in the case of the Houk–List model, are at variance. The hybrid meta-GGA functionals are known to produce errors in reactions involving "π-to-σ bond change" (ca. 2.7 kcal mol^{-1}[31]). The present discrepancy could perhaps be attributed to such known limitations. Furthermore, this functional is predominantly calibrated against thermodynamic, not kinetic, quantities such as those reported here.

[23] The optimized geometries of solvent (or base)-assisted conversion of **3** to **4** or **8** are provided in Figure S5 in the Supporting Information.

[24] The optimized TS geometries for additional stereochemical possibilities are provided in Figure S7 in the Supporting Information.

[25] a) In fact, *syn* addition in the oxazolidinone pathway, in which the electrophile approaches from the same side of the carboxylate group, is about 6 to 10 kcal mol^{-1} higher in energy. b) See Tables S6 and S7 and Figure S8 in the Supporting Information.

[26] The TSs for the addition of **8b** are generally higher in energy by about 2.2 kcal mol^{-1}. See also Table S5 in the Supporting Information.

[27] The % *de* (*anti*:*syn*) is calculated using the relative populations of the most preferred TSs, namely **TS(8a–9a)***si–re*$_{(300)}$ and **TS(8a–9a)***si–si*$_{(180)}$, responsible for the diastereomeric products.

[28] See Tables S6 and S7 in the Supporting Information for further details.

[29] Further details on other possible geometries of **9a**/**9b** are provided in Figure S9 and Tables S9 and S10 in the Supporting Information.

[30] In fact, the protonation of **8** by $[HNMe_3]^+$ to yield **4** is thermodynamically downhill by about 12 kcal mol^{-1} in the solvent phase.

[31] S. E. Wheeler, A. Moran, S. N. Pieniazek, K. N. Houk, *J. Phys. Chem. A* **2009**, *113*, 10376 – 10384.

[32] Gaussian 03 (Revisions C.02/E.01), M. J. Frisch et al., Gaussian, Inc., Wallingford, CT, **2004** (see Computational Methods in the Supporting Information for full citation).

